PROCEEDINGS OF SPIE

Experimental verification of high-NA imaging simulations using SHARP

Davydova, Natalia, Liu, Fei, Benk, Markus, van Setten, Eelco, Bottiglieri, Gerardo, et al.

Experimental verification of high-NA imaging simulations using SHARP

Natalia Davydova[1], Fei Liu[1], Markus Benk[2], Eelco van Setten[1], Gerardo Bottiglieri[1], Anton van Oosten[1], John McNamara[1], Vincent Wiaux[3], Joern-Holger Franke[3], Kenneth Goldberg[2], DS Nam[1], Joseph Zekry[1], Patrick Naulleau[2], Timon Fliervoet[1], Rene Carpaij[1]

[1] ASML Netherlands B.V., De Run 6501, 5504 DR Veldhoven, The Netherlands
[2] Center for X-Ray Optics, Lawrence Berkeley National Laboratory, 1 Cyclotron Rd, Berkeley, CA 94720, United States
[3] IMEC, Kapeldreef 75, B-3001 Leuven, Belgium

ABSTRACT

The next-generation high-NA EUV scanner is being developed to enable patterning beyond the 3-nm technology node. Design and development of the scanner are based on rigorous litho-simulations. It is important to verify key imaging simulation findings by means of aerial image experiments with representative high-NA scanner characteristics. The first ASML-SHARP joint experiment was done with lines and spaces with pitches down to 16 nm wafer scale (1x). The experimental results confirmed the key litho-simulation findings: central obscuration's impact on high-NA imaging and mitigations of obscuration's impact using flex illuminations.

Key words: high NA, EUV lithography, imaging, SHARP, central obscuration, flex illumination, zoneplate

1. INTRODUCTION

To extend Moore's law further throughout next decades, the next-generation high-NA EUV scanner is being developed as a successor to current NXE machines [1, 2]. Novel anamorphic optics design is used in the high-NA scanner to make sure high reflectivity at reticle. Another distinct design feature of the high-NA scanner is that a central obscuration is introduced in the projection optics to reduce the range of reflection angles from the second to the last mirror [1, 2]. Previous litho-simulations have investigated the central obscuration's impact on imaging and proposed mitigations using flex illuminations [3, 4]. The goal of this work is to verify the key imaging simulation findings, by means of aerial image experiments with representative high-NA scanner characteristics.

The Sharp High-NA Actinic Reticle review Project (SHARP) is an EUV photomask microscope at the Center for X-ray Optics in Berkeley [5-7]. The illuminator in SHARP synthesizes source-angular spectra and emulates the illumination conditions in high-NA EUV scanners. Aerial images are formed using a zoneplate lens matched to the mask side numerical aperture of the 0.55-NA projection optics of the EUV scanner. Images of the experiment sites on the mask are projected on a CCD camera at a magnification of 1250x. There is no photoresist involved in image formation. This approach allows studying optical effects separate from resist effects. In particular, mask 3D effects can be investigated, such as best focus shifts through pitch. The first ASML-SHARP joint experiment was done with lines and spaces with pitches down to 16 nm on wafer scale (1x). The experimental results confirmed the key litho-simulation findings:

- Central obscuration can have a negative impact on NILS of intermediate pitches in a through pitch case;
- The negative impact can be repaired by using obscuration-aware illuminations.

Confidential

2. EXPERIMENTAL SETUP

The simplified SHARP setup is shown in Figure 1. The EUV light is from synchrotron and its wavelength is tunable from 13.2 to 13.7 nm with $\Delta\lambda/\lambda$ tunable from 1/900 to 1/1500. The illuminator in SHARP synthesizes source-angular spectra and emulates the anamorphic illumination conditions in high-NA EUV scanners. Aerial images are recorded with an off-axis zoneplate lens matched to the mask side numerical aperture of the 0.55-NA projection optics of the EUV scanner. Images of the experiment sites on the mask are projected on a CCD camera (PIXIS-XO) at a magnification of 1250x. By making use of the chromatic focal-length dependence of the zoneplate lens, the through-focus image data acquisition are achieved by wavelength tuning in small steps [8].
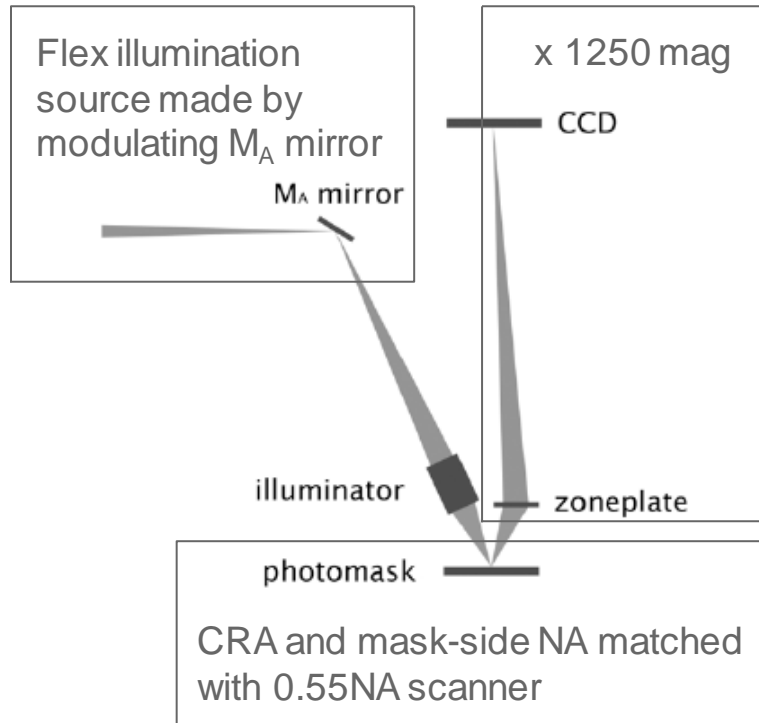
Figure 1. Simplified SHARP setup. Illustration is not to scale.

For our experiment, we used the ORFEO mask which was designed by IMEC, specially for SHARP application. The ORFEO mask includes both isomorphic and anamorphic patterns. The previous imaging experimental results showed good match with simulation results on best focus shift trends through pitch, using zoneplate lens without central obscuration [9]. In our experiments, zoneplate lenses with central obscuration are used for the first time. We selected three different mask sites with anamorphic patterns for measurements with different illumination modes, as shown in Figure 2. "R-0" site includes horizontal L/S patterns P16CD8, P32CD16 and P80CD20. "AR-0" site includes horizontal L/S patterns P24CD12, P32CD16 and P80CD20. "AS-0" site includes vertical L/S patterns P24CD12, P32CD16 and P80CD20. We do not consider vertical P16 as it is not resolved on mask. The raw aerial images of "AR-0" site at best focus measured with dipole and Source 2 illumination are shown in Figure 3. The differences on the image contrast for P32CD16 (right H lines) and P80CD20 (left H lines) is clearly visible.
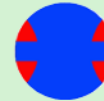
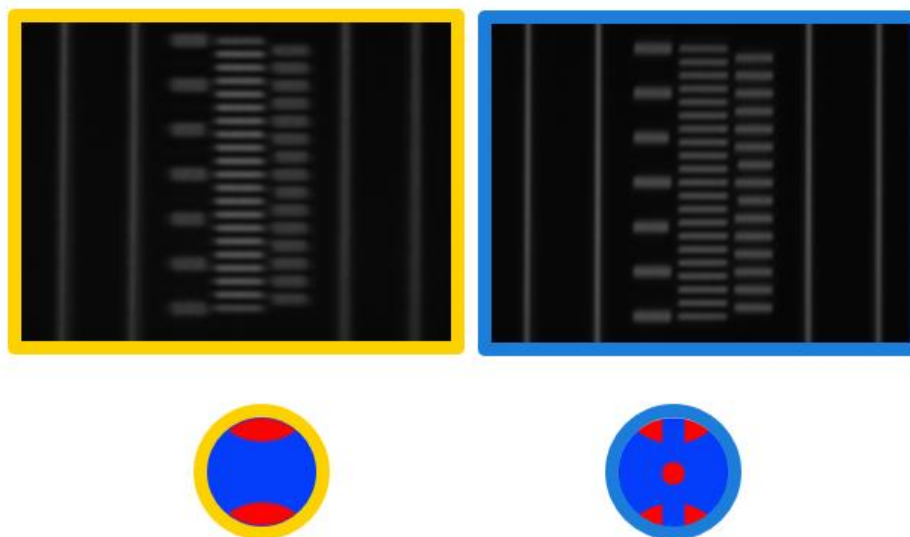*Figure 2. Illumination modes and L/S patterns used in SHARP experiments*

Figure 3. Raw aerial images of "AR-0" site at best focus with dipole and Source 2 illumination

3. MEASUREMENT REPEATABILITY

Before we use SHARP measurement data to draw any conclusions, we would like to verify repeatability of the measured results. The metric we evaluate is the maximal Normalized Image Log-Slope (NILS) through focus for each set of measurement.

First, the repeatability is assessed by repeating measurements using the same pattern, same mask site, same illumination, same zoneplate lens with central obscuration at a different time of the day.

For horizontal features, the repeatability variation increases with decreasing pitch: going from 0.8% for P80CD20 to 8.1% for P16CD8, as shown in Figure 4 and Table 1. For vertical features through pitch, the relative change between the repeated measurements is less than 1%.
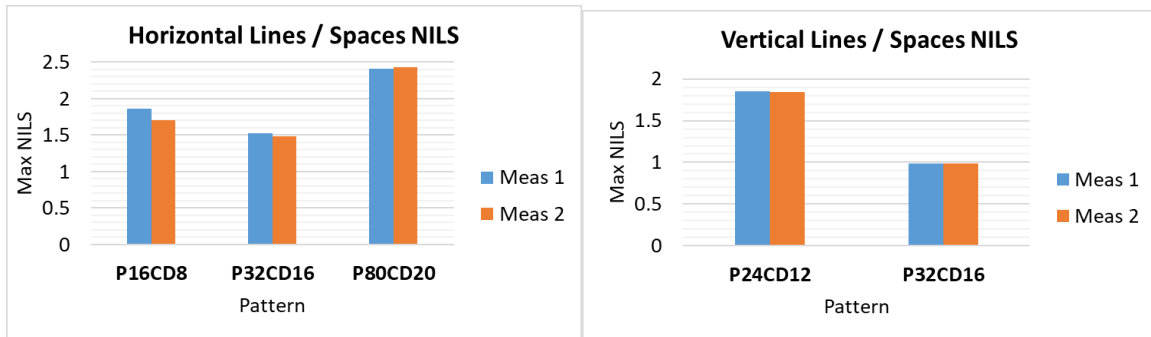
Figure 4. Max NILS for horizontal (left) and vertical (right) features through pitch, 1ˢᵗ measurement vs repeated measurement

Table 1. Repeatability test results with horizontal L/S through pitch

Max NILS	Measurement 1	Measurement 2	Relative change
Pitch 16 CD8 Horizontal	1.86	1.71	-8.1%
Pitch 32 CD16 Horizontal	1.53	1.48	-3.3%
Pitch 80 CD20 Horizontal	2.41	2.43	0.8%
Pitch 24 CD12 Vertical	1.85	1.84	-0.5%
Pitch 32 CD16 Vertical	0.99	0.99	0 %

Secondly, the repeatability is evaluated by repeating the measurements using the same pattern, different mask site, same illumination at different time of the day. Max NILS of P32CD16 (H) feature with obscuration showed repeatability ~4% , comparable to the results in Table 1. Without obscuration, the relative change is about 0.5%.
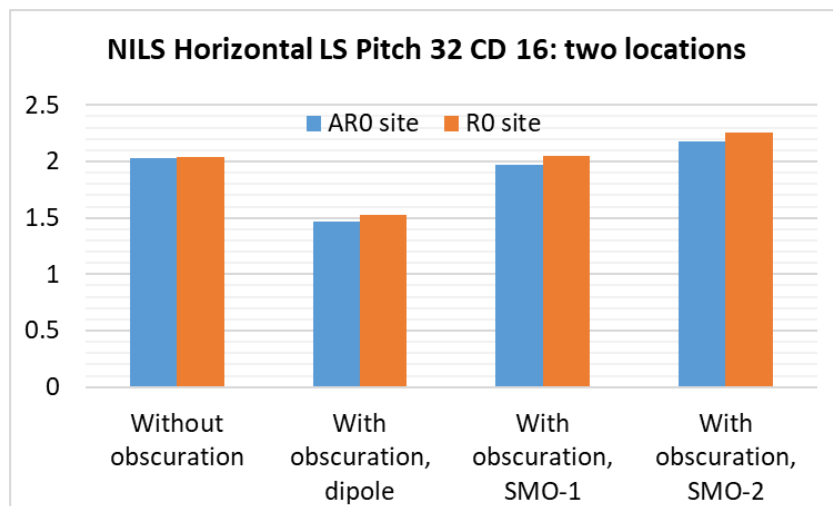

Figure 5. Max NILS for the same P32CD16(H) pattern, same illumination, with different mask sites

Table 2. Repeatability test results with P32CD16 (H) with the same illumination in two different sites on reticle.

Max NILS of P32CD16 (H)	AR0 site	R0 site	Relative change in %
Without obscuration	2.03	2.04	0.5%
With obscuration, dipole	1.47	1.53	4.1%
With obscuration, Source 1	1.97	2.05	4.1%
With obscuration, Source 2	2.18	2.26	3.7%

For all subsequent bar graphs showing max NILS, we use 8% as the error of the measurements.

4. SCANNER SIMULATIONS VS SHARP EXPERIMENTS

The simulation results shown further in this work are done for the ideal High NA scanner and not for SHARP tool, there are some significant differences, some of them are shown in Table 3.

Table 3. Differences between SHARP and Hyperlith scanner simulations.

Parameter	SHARP experiment	Hyperlith scanner simulations
Magnification	1250x	1/4x in X, 1/8x in Y
Polarization	X – polarized	Unpolarized
Mask absorber	60 nm 58 nm TaBN + 2 nm TaBO	55.3 nm (optimized for HighNA) 41.3 nm TaBN + 14 nm TaBO
Illumination source	Fourier synthesized angular spectra, not perfectly uniform	Flat top illumination, perfectly uniform
Vibrations	possible	none

Especially, polarization can have a large impact. X-polarization is bad for vertical features which can explain low measured NILS values.

5. CENTRAL OBSCURATION IMPACT ON NILS

The high-NA scanner has central obscuration of approximately 20% of the pupil plane. Previous simulation results showed that the central obscuration can have a negative impact on NILS for P32CD16 L/S, in which case the +/- 1st order diffracted light is partially blocked by the central obscuration, as illustrated in Figure 6 [3,4].
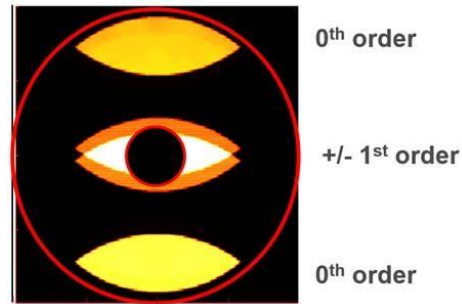
Figure 6. Pupil image with the diffracted orders of dipole illumination from horizontal P32CD16 L/S

We compare measured and simulated results in this and the following chapters in the following way (Figure 7): the empty bars represent simulated max NILS and filled bars represent measured values. We see immediately that measured NILS is lower. This is expected as possible SHARP tool vibrations and aberrations are not taken into account in simulations. As we have indicated in the previous chapter, X-polarization has additional negative impact on vertical structures.

The small cartoons above the bars show the diffraction pattern and its interaction with the obscuration area.

The table underneath the bar chart (Table 4) shows relative NILS differences caused by obscuration as expected in simulation and as measured in the experiment.

As expected from the simulations, pitch 16 does not feel obscuration as its diffraction orders do not pass through it. The measurements confirm this observation.

For pitch 24, the first diffraction order is slightly obscured, such that we expect a small NILS drop of about 5%. This is confirmed by measurements for the horizontal orientation. The measured NILS drop for vertical orientation is however much larger, up to 20%. This is not expected. A possible explanation can be a larger obscuration area in the experiment or a displacement of obscuration in x-direction. This will be investigated further.

For pitch 32, we expect a NILS drop of about 30%. This is confirmed by measurements. The match is almost perfect for the Horizontal orientation. For the vertical orientation, we see a smaller effect than expected.
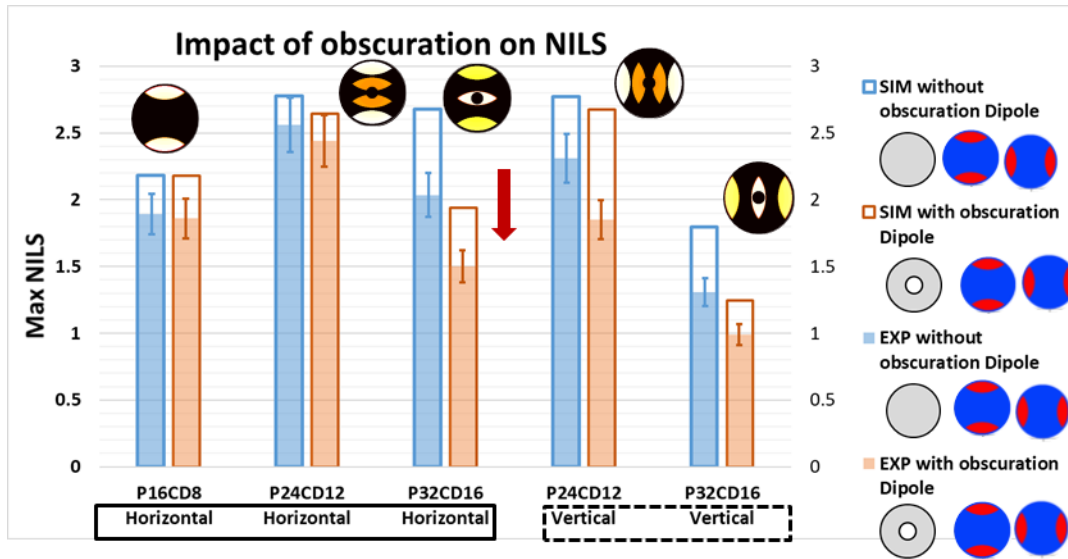
Figure 7. Negative impact of central obscuration demonstrated for horizontal features

Table 4. Comparison of NILS drop in Experiment vs Simulations

Obscuration impact on NILS, %	P16CD8 Horizontal	P24CD12 Horizontal	P32CD16 Horizontal	P24CD12 Vertical	P32CD16 Vertical
Simulation	0%	-4.9%	-27%	-4%	-31%
Experiment	-1.6%	-4.7%	-28%	-20%*	-24%

The full NILS through focus curves are shown in Figure 8, Figure 9, Figure 10 for the three measurement sites with and without obscuration. These detailed data are also used for best focus determination which we report in a subsequent chapter. Also NILS curvature can be extracted from the data; we have not considered this metric further though it can be used to assess the NILS-based usable depth of focus.
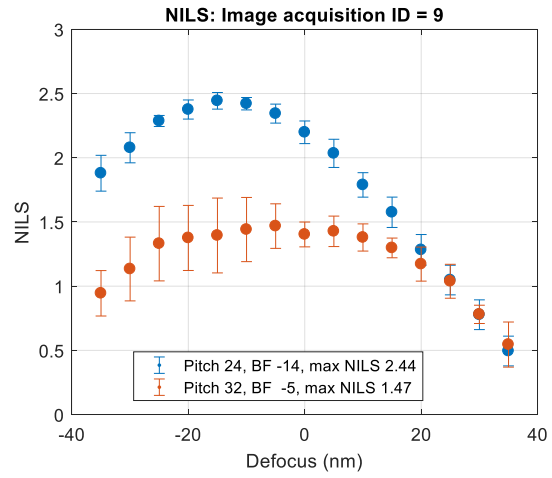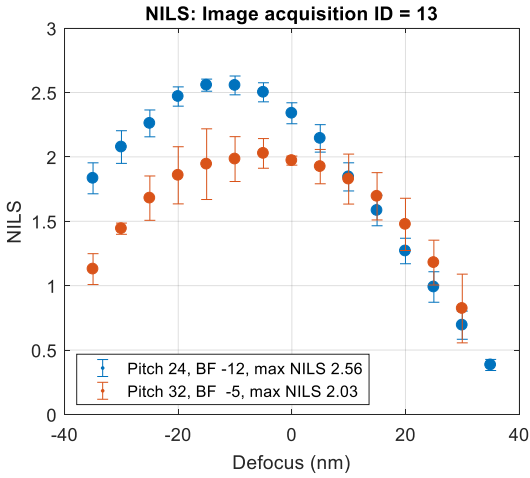
Figure 8. NILS through focus measured with AR0 site horizontal L/S with dipole illumination. Left: without obscuration. Right: with obscuration.
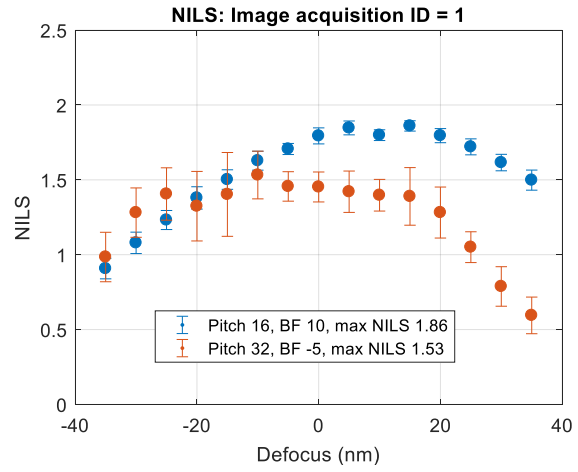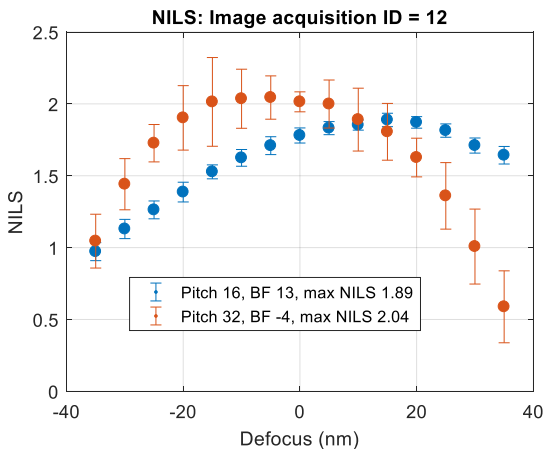

Figure 9. NILS through focus measured with R0 site horizontal L/S with dipole illumination. Left: without obscuration. Right: with obscuration.

Proc. of SPIE Vol. 11517 1151714-8

Downloaded From: https://www.spiedigitallibrary.org/conference-proceedings-of-spie on 20 Oct 2020
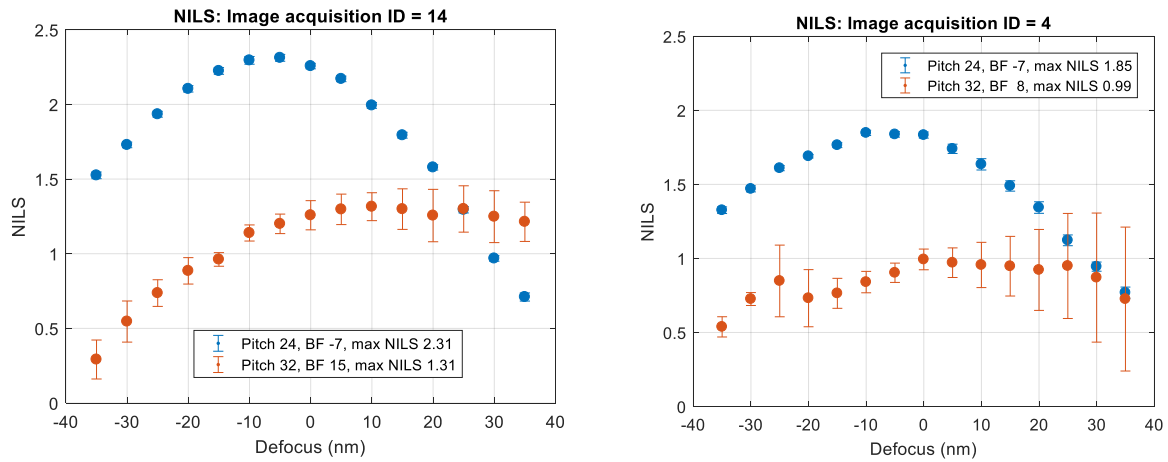Terms of Use: https://www.spiedigitallibrary.org/terms-of-use

Figure 10. NILS through focus measured with AS0 site vertical L/S with dipole illumination. Left: without obscuration. Right: with obscuration.

6. MITIGATION USING FLEX ILLUMINATION AVOIDING OBSCURATION (Source 1)

Simulation results showed that by removing the illumination source pixels, of which the +/- 1st diffracted light is blocked by the central obscuration, the NILS can be improved. SHARP experiment has clearly demonstrated this effect for pitch 32 (Figure 11 and Table 5), showing NILS compensation to almost the same value as it was without obscuration (-3%) for horizontal features. For vertical features the compensation is smaller than expected, the NILS value is still 17% lower than it was without obscuration.

For pitch 16 there is a slight loss of contrast which is within the error bar.

For vertical pitch 24 the compensation is not observed. This shows that further root cause analysis and setup improvements are required for this orientation. This will be investigated in more detail.
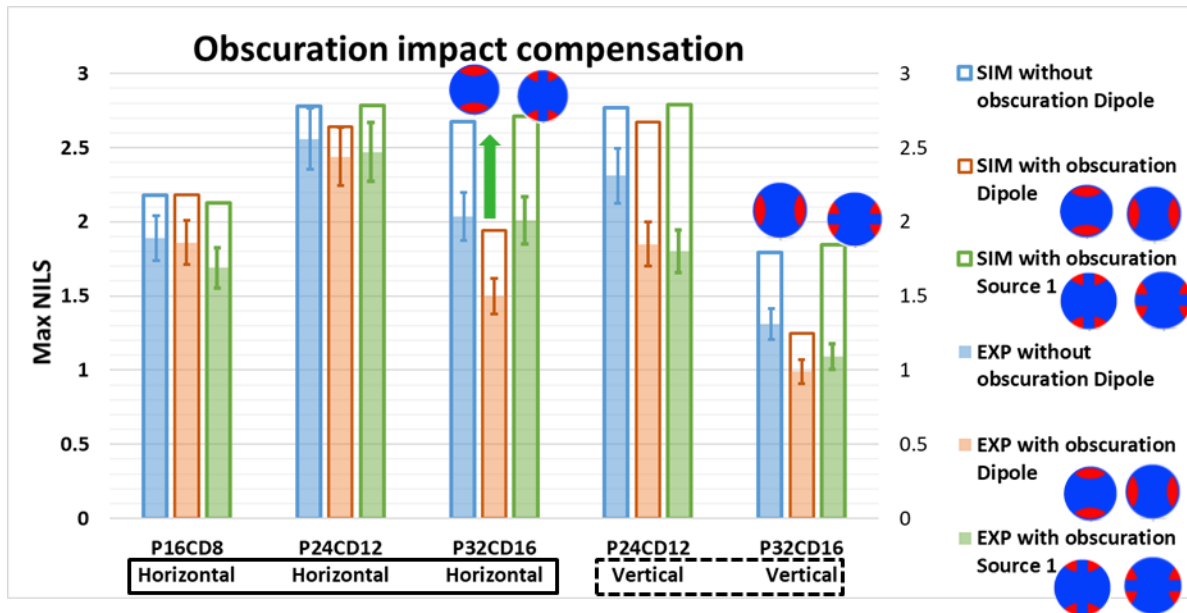

Figure 11. Flex illumination mitigation demonstrated for P32CD16 (H)

Table 5. For horizontal features, the trends from experiments match with simulations

NILS change in % Obscuration Source 1	P16CD8 Horizontal		P24CD12 Horizontal		P32CD16 Horizontal		P24CD12 Vertical		P32CD16 Vertical	
Simulation	0	-2	-5	0	-27	+1	-4	+1	-31	+3
Experiment	-1.6	-11	-5	-4	-28	-3	-20	-22	-24	-17
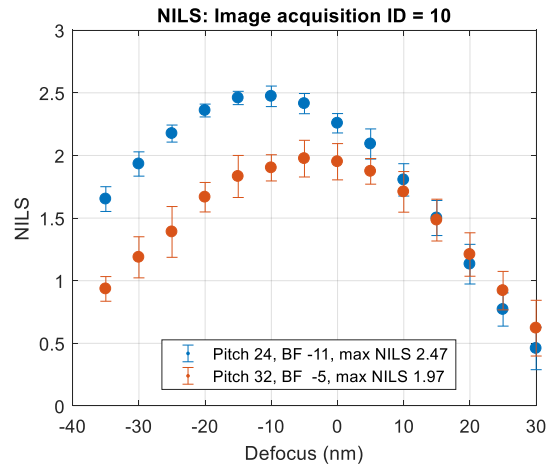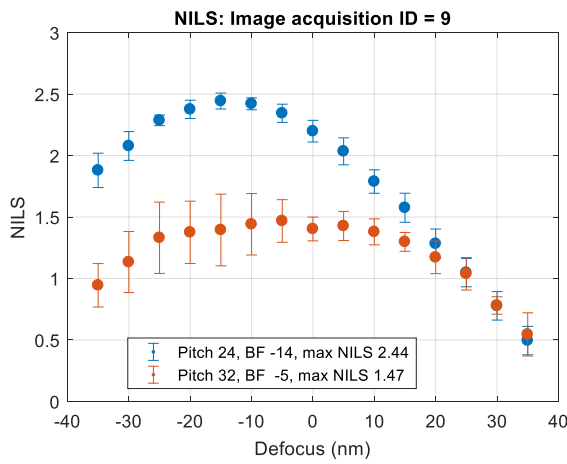
Figure 12. NILS through focus measured with AR0 site horizontal L/S with central obscuration. Left: with dipole. Right: with Source 1.
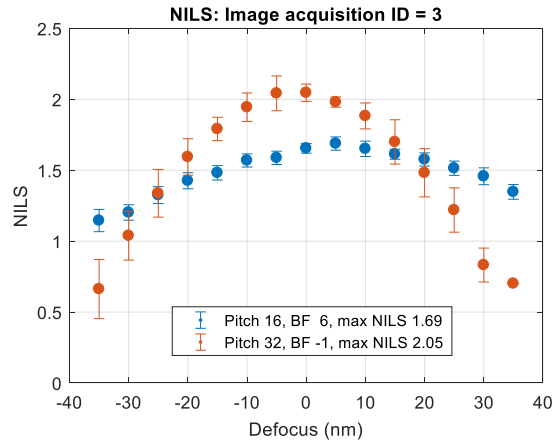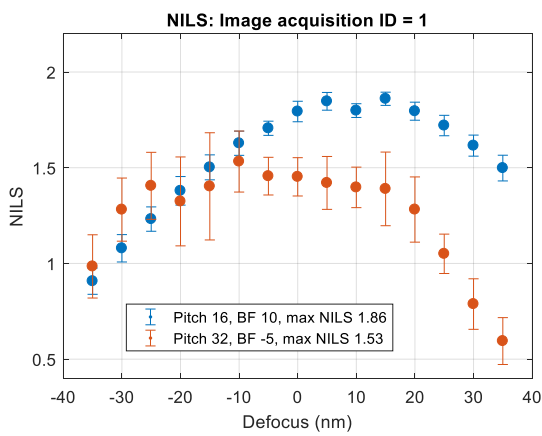

Figure 13. NILS through focus measured with R0 site horizontal L/S with central obscuration. Left: with dipole. Right: with Source 1.
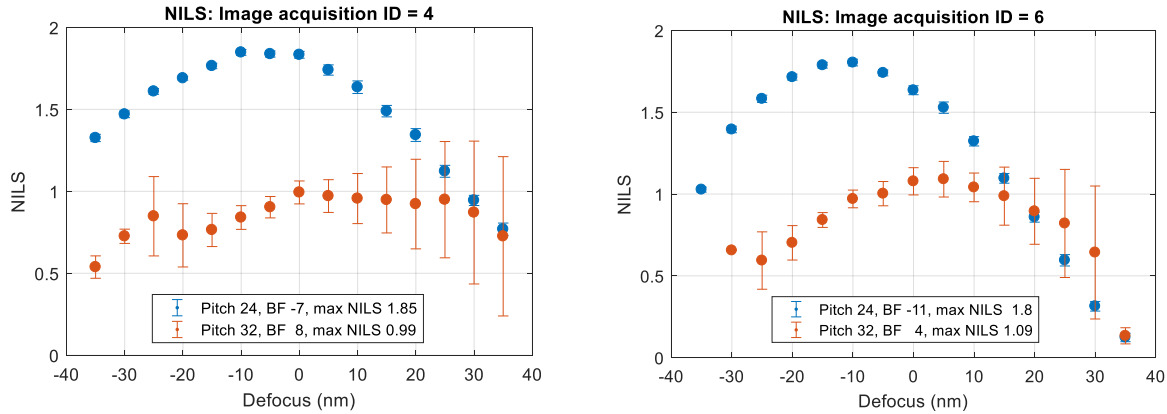
Figure 14. NILS through focus measured with AS0 site vertical L/S with central obscuration. Left: with dipole. Right: with Source 1

7. PUTTING LIGHT IN OBSCURATION (Source 2)

Previous simulation work showed that adding source pixels in the central obscuration can produce partially frequency-doubled aerial images with increased NILS [3]. Experimental data confirmed this effect by showing 10% NILS improvement for P32CD16 (H) and 6% for P32CD16 (V).

Especially large NILS gain is observed for an isolated pitch 80 targeted to 20 nm lines which is in accordance with the expectations though detailed simulations are pending.

For pitch 16 we observe a NILS drop which is not understood as this pitch should be blind to the light put in obscuration as it is diffracted outside NA. For pitch 24 there is also a NILS drop.

For this illumination settings we still need to do more detailed data analysis and simulations in order to estimate NILS loss vs NILS gain.
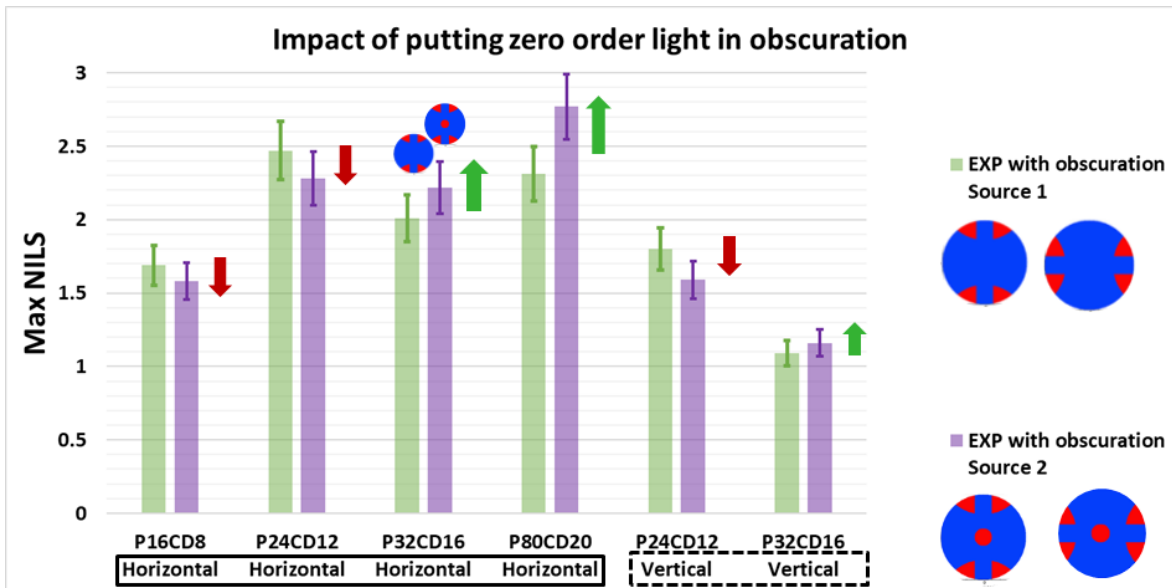

Figure 15 Flex illumination mitigation demonstrated for P32CD16 (H)

Table 6. For P32CD16 (H), experiment showed adding light in the obscuration improves NILS, as expected

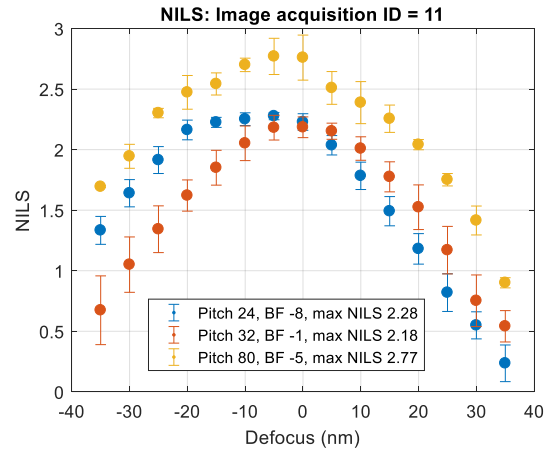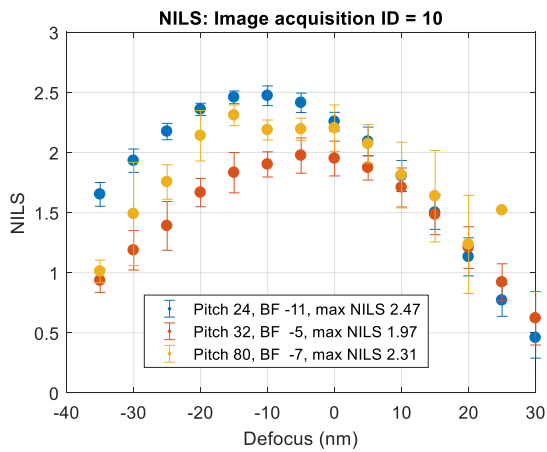| NILS change, % Source 2 w.r.t. Source 1	P16CD8 Horizontal	P24CD12 Horizontal	P32CD16 Horizontal	P80CD20 Horizontal	P24CD12 Vertical	P32CD16 Vertical
Experiment	-7	-8	+10	+20	-12	+6

Figure 16. NILS through focus measured with AR0 site horizontal L/S with central obscuration. Left: with Source 1. Right: with Source 2.
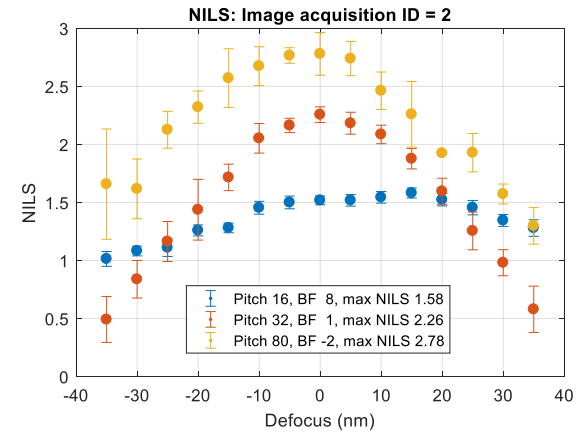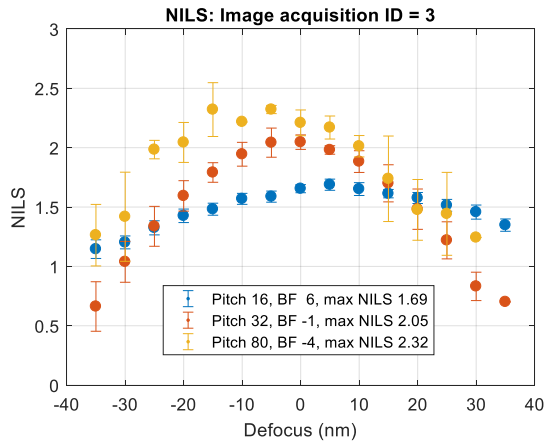

Figure 17. NILS through focus measured with R0 site horizontal L/S with central obscuration. Left: with Source 1. Right: with Source 2.
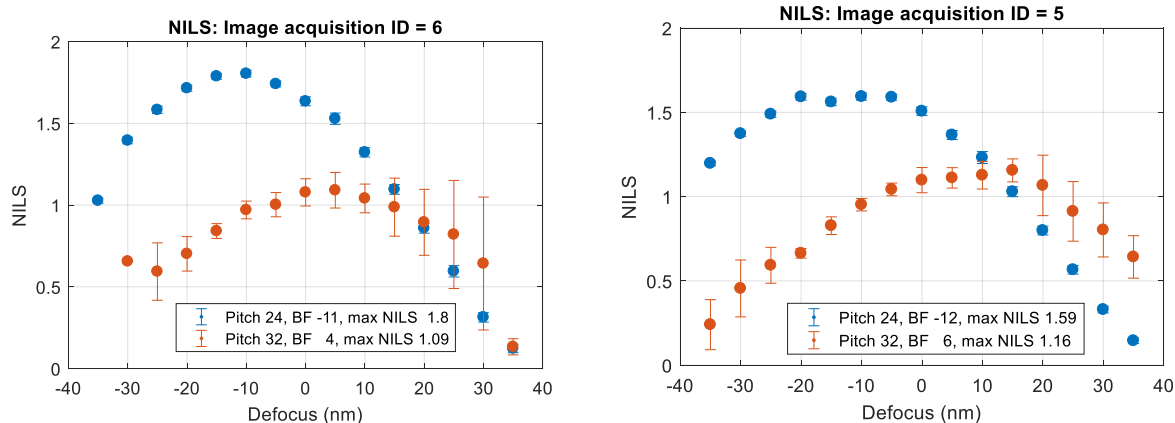
Figure 18. NILS through focus measured with AS0 site vertical L/S with central obscuration. Left: with Source 1. Right: with Source 2.

8. NILS CORRELATION BETWEEN SIMULATIONS AND EXPERIMENTS

In the previous chapters, the absolute NILS difference between SHARP experiment and Hyperlith scanner simulations is observed. We collected all measured and simulated data points in one correlation graph (Figure 19). It shows good correlation on large range of NILS variation which means that we capture significant contrast changes. Horizontal and vertical features show different correlation between measurements and simulations, probably partially due to impact of polarization. For horizontal features, the correlation slope is close to 1 which means that the magnitude of the changes is matched. For vertical features, an improvement is required.
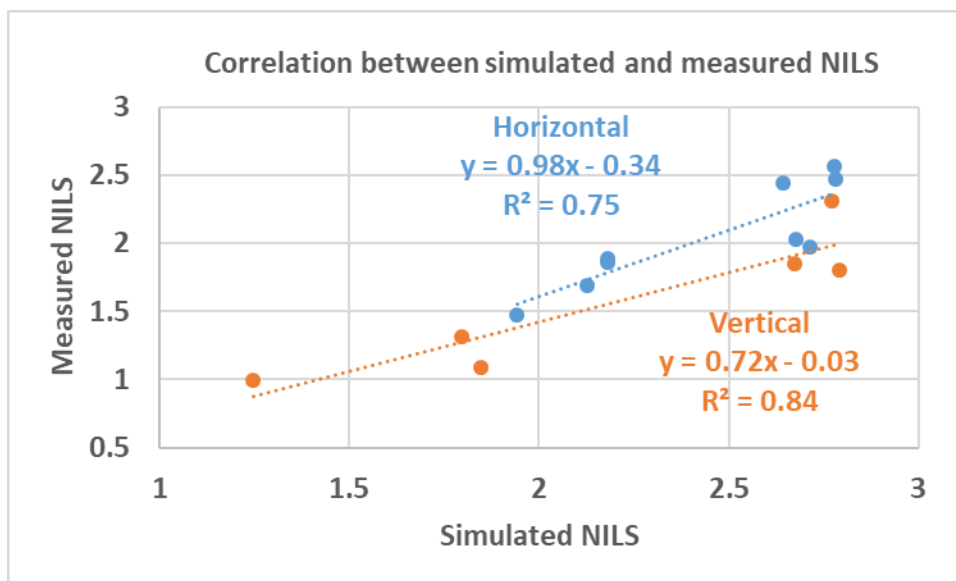

Figure 19 NILS correlation between experiment and simulations

9. BEST FOCUS SHIFT

From the NILS-based focus curve, we can determine the best focus (BF) for each pattern. The relative best focus shift between different pitches can then be compared to the simulated results (Figure 20). The relative trends are confirmed. There is almost a perfect BF match between measurements and simulations

for horizontal P24-P32, though experimental values for vertical P24-P32 shifts are 5-8 nm larger than simulated and also, for horizontal P16-P32, experimental BF shifts are 3-5 nm larger. We notice an additional benefit of using the obscuration aware source for horizontal features (blue and orange lines): the best focus shifts between the pitches are reduced with respect to the dipole illumination.
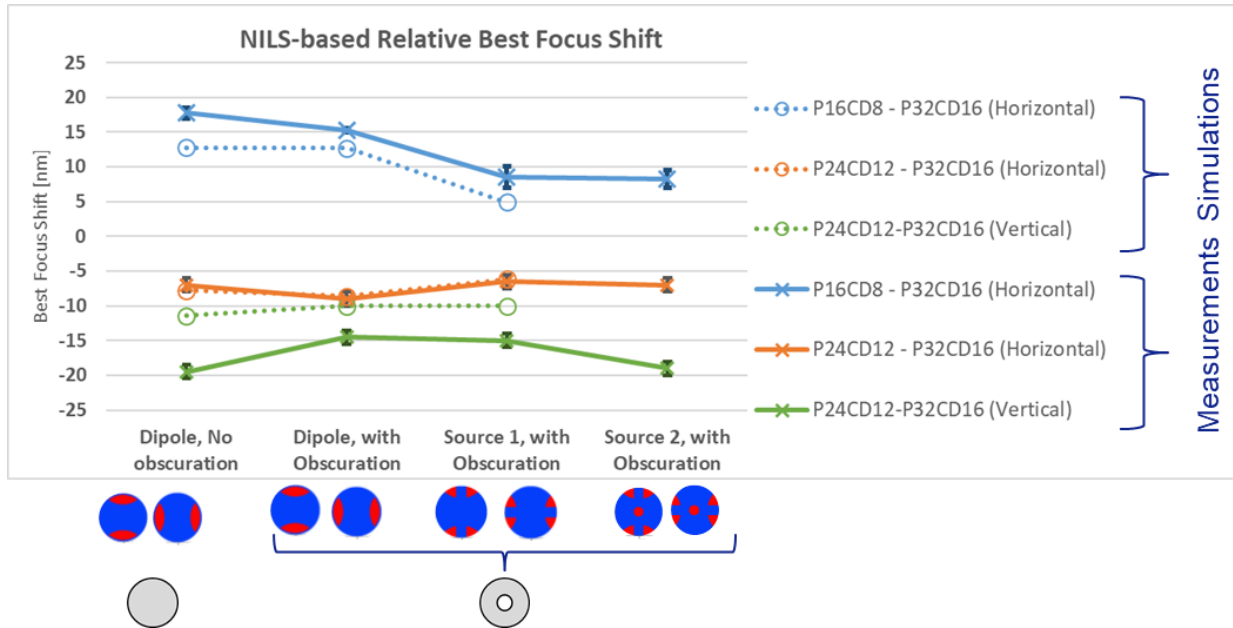

Figure 20. Measured and simulated relative best focus shift of P16 and P24 with respect to P32 for four illumination settings.

10. CONCLUSIONS

The 1st ASML-SHARP experiment is done to gain more confidence on litho-simulation and its prediction on the imaging performance of high-NA machines. With its unique capability to make flexible illuminations and anamorphic zoneplate objective lenses, SHARP proves to be a useful tool for high-NA litho-simulation trend verification.

For NILS measurements SHARP repeatability error is maximum 8%, typically smaller.

The experimental results confirmed key litho-simulation findings:

1) central obscuration has a negative impact on NILS if the first diffracted order is partially blocked by obscuration. It is demonstrated in experiment for P32. The NILS drop of about 30% is observed;
2) The negative impact can be compensated by using flex illumination (avoiding obscuration). It is demonstrated for P32: NILS comes back to the level it was without obscuration;
3) Illumination with light in obscuration helps to increase NILS for intermediate and isolated pitches. It is demonstrated for P32 and P80, though a NILS drop for small pitches is to be understood;
4) Relative best focus shift trend matches with simulations.

We summarize NILS results for horizontal pitch 32 in Figure 21 and we would like to conclude with a take away message: for metal layers with small base pitch (< ~20 nm) and intermediate pitches (~2x base pitch) the interaction of diffraction orders with obscuration must be taken into account in High NA source optimization.
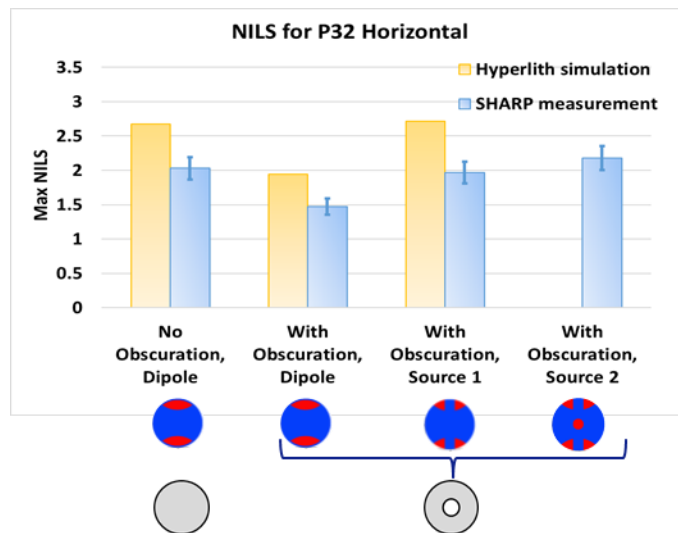
Figure 21. Simulated and measured NILS for horizontal pitch 32 summarized for all source and obscuration settings.

11. ACKNOWLEDGEMENTS

12. REFERENCE

[1] J. van Schoot, K. Troost, F. Bornebroek, R. van Ballegoij, S. Lok, et al., "High-NA EUV lithography enabling Moore's law in the next decade," Proc. SPIE 10450, 104500U (2017)

[2] C. Zahlten, P. Gräupner, J. van Schoot, P. Kürz, J. Stoeldraijer, W. Kaiser, "High-NA EUV lithography: pushing the limits," Proc. SPIE 11177, 35th European Mask and Lithography Conference (EMLC 2019)

[3] E. van Setten, G. Bottiglieri, J. McNamara, J. van Schoot, K. Troost, J. Zekry, T. Fliervoet, S. Hsu, J. Zimmermann, M. Roesch, B. Bilski, P. Graeupner, "High NA EUV lithography: Next step in EUV imaging," Proc. SPIE 10957, Extreme Ultraviolet (EUV) Lithography X, 1095709 (2019)

[4] E. van Setten, G. Bottiglieri, L. de Winter, J. McNamara, P. Rusu, J. Lubkoll, G. Rispens, J. van Schoot, J. Timo Neumann, M. Roesch, B. Kneer, "Edge placement error control and Mask3D effects in High-NA anamorphic EUV lithography," Proc. SPIE 10450, International Conference on Extreme Ultraviolet Lithography 2017, 104500W (2017)

[5] K. A. Goldberg, I. Mochi, S. B. Rekawa, N. S. Smith, J. B. Macdougall, P. P. Naulleau, "An EUV Fresnel zoneplate mask-imaging microscope for lithography generations reaching 8 nm," Proc. SPIE 7969, Extreme Ultraviolet (EUV) Lithography II, 796910 (2011)

[6] M. Benk, A. Wojdyla, W. Chao, F. Salmassi, S. Oh, Y.-G. Wang, R. Miyakawa, P. Naulleau, and K. Goldberg, "Emulation of anamorphic imaging on the SHARP extreme ultraviolet mask microscope, " J. Micro. Nanolithogr. MEMS MOEMS 15 (3), 033501 (2016)

[7] M. Benk, W. Chao, R. Miyakawa, K. Goldberg, P. Naulleau, "Upgrade to the SHARP EUV mask microscope," Proc. SPIE 10957, Extreme Ultraviolet (EUV) Lithography X, 109570V (2019)

[8] K. A. Goldberg, I. Mochi, S. Huh, "Collecting EUV mask images through focus by wavelength tuning," Proc. SPIE 7271, Alternative Lithographic Technologies, 72713N (2009)

[9] V. Wiaux, V. Philipsen, E. Hendrickx "Mask 3D effects experimental measurements with NA 0.55 anamorphic imaging (Conference Presentation)", Proc. SPIE 10809, International Conference on Extreme Ultraviolet Lithography 2018, 1080913 (2018)